Journal of Hazardous Materials 191 (2011) 380–387

Contents lists available at ScienceDirect

Journal of Hazardous Materials

journal homepage: www.elsevier.com/locate/jhazmat

Consequence of chitosan treating on the adsorption of humic acid by granular activated carbon

Sh. Maghsoodloo[a], B. Noroozi[a,*], A.K. Haghi[a], G.A. Sorial[b]

[a] Department of Textile Engineering, University of Guilan, P.O. Box 41635-3756, Rasht, Iran
[b] Environmental Engineering and Science Program, School of Energy, Environmental, Biological, and Medical Engineering, University of Cincinnati, P.O. Box 210012, Cincinnati, OH 45221-0012, USA

ARTICLE INFO

Article history:
Received 8 February 2011
Received in revised form 17 April 2011
Accepted 23 April 2011
Available online 5 May 2011

Keywords:
Activated carbon
Adsorption
Chitosan
Humic acid
Natural organic matter (NOM)

ABSTRACT

In this work, equilibrium and kinetic adsorption of humic acid (HA) onto chitosan treated granular activated carbon (MGAC) has been investigated and compared to the granular activated carbon (GAC). The adsorption equilibrium data showed that adsorption behaviour of HA could be described reasonably well by Langmuir adsorption isotherm for GAC and Freundlich adsorption isotherm for MGAC. It was shown that pre-adsorption of chitosan onto the surface of GAC improved the adsorption capacity of HA changing the predominant adsorption mechanism. Monolayer capacities for the adsorption of HA onto GAC and MGAC were calculated 55.8 mg/g and 71.4 mg/g, respectively. Kinetic studies showed that film diffusion and intra-particle diffusion were simultaneously operating during the adsorption process for MGAC.

1. Introduction

Soil organic matter (SOM) refers to all organic carbon containing substances in soils [1]. SOM is usually classified into non-humic and humic substances (HS). A major component of SOM and natural organic matter (NOM), consist of HS. They are yellow to black in colour, high persistent to chemical and biological degradation and are non-volatile. They are formed through aerobic and anaerobic decomposition of plant and animal material detritus [2]. HA is one of the major components of HS which arise by the microbial degradation of biomolecules [3]. The presence of HA in water is not directly toxic but has undesirable effects on the appearance and taste of water and could lead to undesired and hazardous products which are known as disinfectant by products in water treatment after disinfection [4,5]. HA can affect water quality adversely by the undesirable colour (at concentrations above 5 mg/L), odour and taste [4,6], serve as food for bacterial growth, and trap heavy metals, pesticides and herbicides [7–9] which causes contamination of ground and surface water due to excess limits of their acceptable concentrations [10]. Different methods applied for remediation of humic substances include ozonation, biofiltration [11], membrane technology [12], coagulation [13], flotation [2], ion-exchange [14,15] and adsorption [16]. Adsorption is usually the simplest and most cost-effective technique [5]. Removal of NOM or its degradation to less reactive products is a priority task in water treatment, among which adsorption comprises an important portion [16]. Activated carbons (ACs) are the most widely used adsorbents to remove contaminants from wastewater because of its extended surface area, microporous structure, high adsorption capacity and high degree of surface reactivity [17]. In recent years, several investigations have been reported on adsorption behaviour of heavy metal–HAs on some adsorbents such as activated carbon [18,19], clays [1,20], alumina [21], chitin and chitosan [22], fly ash [3,5], zeolite [23], silica [24], activated sludge [25] and hydrophobic surface like cationic surfactants [26].

Chitin and chitosan are recommended as suitable functional materials because these natural polymers have excellent properties such as biocompatibility, biodegradability, non-toxicity, and adsorption properties. Recently, much attention has been made to chitosan as a potential polysaccharide resource. Chitosan, which is at least 50% deacetylated chitin (poly(β-(1-4)-N-acetyl-D-glucosamine), is the only pseudonatural cationic polymer and thus, it finds many applications that follow due to its unique character [27,28]. Chitosan application as biosorbents is justified by its outstanding chelation behaviour [29,30].

HA includes both hydrophobic and hydrophilic components as well as many chemical functional groups such as carboxylic, phenolic, carbonyl, and hydroxyl groups connected with the aliphatic or aromatic carbons in the structure. The existence of carboxylic

* Corresponding author. Tel.: +98 131 6690270; fax: +98 131 6690271.
E-mail addresses: babaknoroozi@guilan.ac.ir, Babak.noroozi@yahoo.com (B. Noroozi).

0304-3894/$ – see front matter © 2011 Elsevier B.V. All rights reserved.
doi:10.1016/j.jhazmat.2011.04.096

Nomenclature

A	Tempkin isotherm constant (L/g)
a_L	Constant in Langmuir isotherm model (L/mg)
B	Tempkin isotherm constant
B_t	Mathematical function of q_t/q_e
C_e	Equilibrium concentration of the adsorbate (mg/L)
C_t	Equilibrium concentration of the adsorbate at time t (mg/L)
C_i	Initial concentration of the adsorbate (mg/L)
F	Fraction of solute adsorbed at different times t
FTIR	Fourier transform infrared
GAC	Granular activated carbon
HA	Humic acid
K	Rate constant of irreversible pseudo first-order kinetic (min^{-1})
K_1	Rate constant of reversible pseudo first-order kinetic (min^{-1})
K_2	Rate constant of pseudo second-order kinetic (g/min mg)
K_f	Constant of Freundlich isotherm $(mg/g)/(mg/L)^{1/n}$
K_L	Constant in Langmuir isotherm model (L/g)
k_p	Rate constant for intra-particle diffusion ($mg/g\ min^{0.5}$)
MGAC	Modified or chitosan treated granular activated carbon
n	Constant of Freundlich isotherm
NOM	Natural organic matter
pH_{pzc}	pH of the point of zero charge
PSD	Pore size distribution
q_e	Amount of solute adsorbed at equilibrium (mg/g)
q_t	Amount of solute adsorbed at time t (mg/g)
R^2	Square of the correlation coefficient
SEM	Scanning electron microscopy
V	Volume of solution used in the adsorption experiment (L)
w	Dry weight of adsorbent (g)

and phenolic groups causes HA to be negatively charged in aqueous solutions [31]. It has been proposed that the structure of HA can undergo different changes from rather linear to coiled or more spherical configurations because of the change of pH and HA concentration [32]. Hence pH will play a major role in the adsorption process.

In this work, the ability of chitosan treatment to improve the features of GAC for the removal of HA has been studied using adsorption experiments. Equilibrium data were correlated by three adsorption isotherm models namely, Langmuir, Freundlich and Tempkin isotherm model. The effect of initial pH of HA solution has been studied. Kinetic experiments have been also conducted to investigate the rate of HA adsorption by GAC and MGAC.

2. Materials and methods

2.1. Materials

HA and chitosan with 85% degree of deacetylation was obtained by Sigma–Aldrich and used without further purification. F400 (Filtrasorb 400) was used as a typical GAC (Calgon, Pittsburg, PA). The adsorbent was dried in the oven at 105 °C overnight to remove any moisture present and then stored in a desiccator until use. The physical properties of GAC F400 were determined by conducting nitrogen adsorption at 77.2 K for determining multipoint specific surface area and the basic t-plot micropore analysis by using

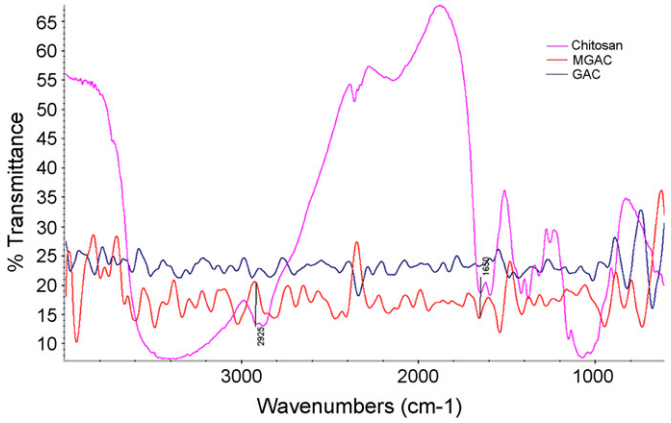

Fig. 1. FTIR spectrum of chitosan, GAC and MGAC.

TriStar 3000 Gas Adsorption Analyzer. The effective PSD for F400 could range from 4 to 800 Å. The pore size distribution of GAC and the obtained results for its physical properties can be found elsewhere [33]. The pH of the point of zero charge pH_{pzc}, i.e. the pH above which the total surface of the carbon particles is negatively charged, was measured for GAC about 9.8 by the so-called pH drift method [34].

2.2. Chitosan treating of GAC

MGAC was prepared as an alternative adsorbent by treating of the GAC with chitosan. Stock solution of the chitosan was prepared as 10 g/L in 1% (v/v) of acetic acid solution. The GAC was immersed in the chitosan solution for 24 h at room temperature. After filtering and washing with distilled water to remove excess chemicals and to obtain neutral pH, the adsorbent was soaked in sodium hydroxide 0.1 M solution in order to precipitate the adsorbed chitosan. After washing out the base, the prepared adsorbent was dried in oven at 80 °C for 6 h and stored in a desiccator until experimental use. FTIR spectrum of the GAC before and after chitosan treating has been evaluated using Nicolet-Mana-560. Also X-ray diffraction analysis has been done by XRD D500, Siemens, Germany, Cu Kα radiation (λ = 1.5405 Å) at 30 kV, 25 mA. Scattering angles ranged from 10° to 80°, with a scanning speed at measuring time of 2° per min.

2.3. Adsorption isotherm and kinetics

Adsorption isotherm experiments for GAC and MGAC were carried out in a batch equilibrium technique at 25 °C. Certain amounts of the adsorbents were contacted with 40 mL of different concentration of HA solutions in the range of 10–100 mg/L in 50 mL capped bottles. The solutions were stirred using a shaker model WB14 of Memmerf, Germany kept under dark conditions. At equilibrium the solutions were centrifuged using Rotana 460R at 3500 rpm and 25 °C for 5 min. A Cintra 10 UV–vis spectrophotometer was used for optical absorbance measurements at maximum wavelength of HA (254 nm) to calculate the adsorbate concentrations. TOC analyzer was used as well as UV–vis in order to confirm no biodegradation of humic acid occurred. In order to investigate the effect of pH on the adsorption of HA, the equilibrium adsorption experiments have been run at three different buffers; pH 4 (17 mL sodium stearate 0.1 M + 33 mL stearate acid 0.1 M dilute to 100 mL), pH 7 (50 mL potassium dihydrogen phosphate 0.1 M + 29.1 mL sodium hydroxide 0.1 M dilute to 100 mL) and pH 10 (50 mL borax 0.1 M + 18.3 mL sodium hydroxide 0.025 M dilute to 100 mL).

Kinetic experiments were carried out by stirring a certain amount of the adsorbents with 500 mL of the solution containing the HA on a magnetic stirrer equipped with temperature controller

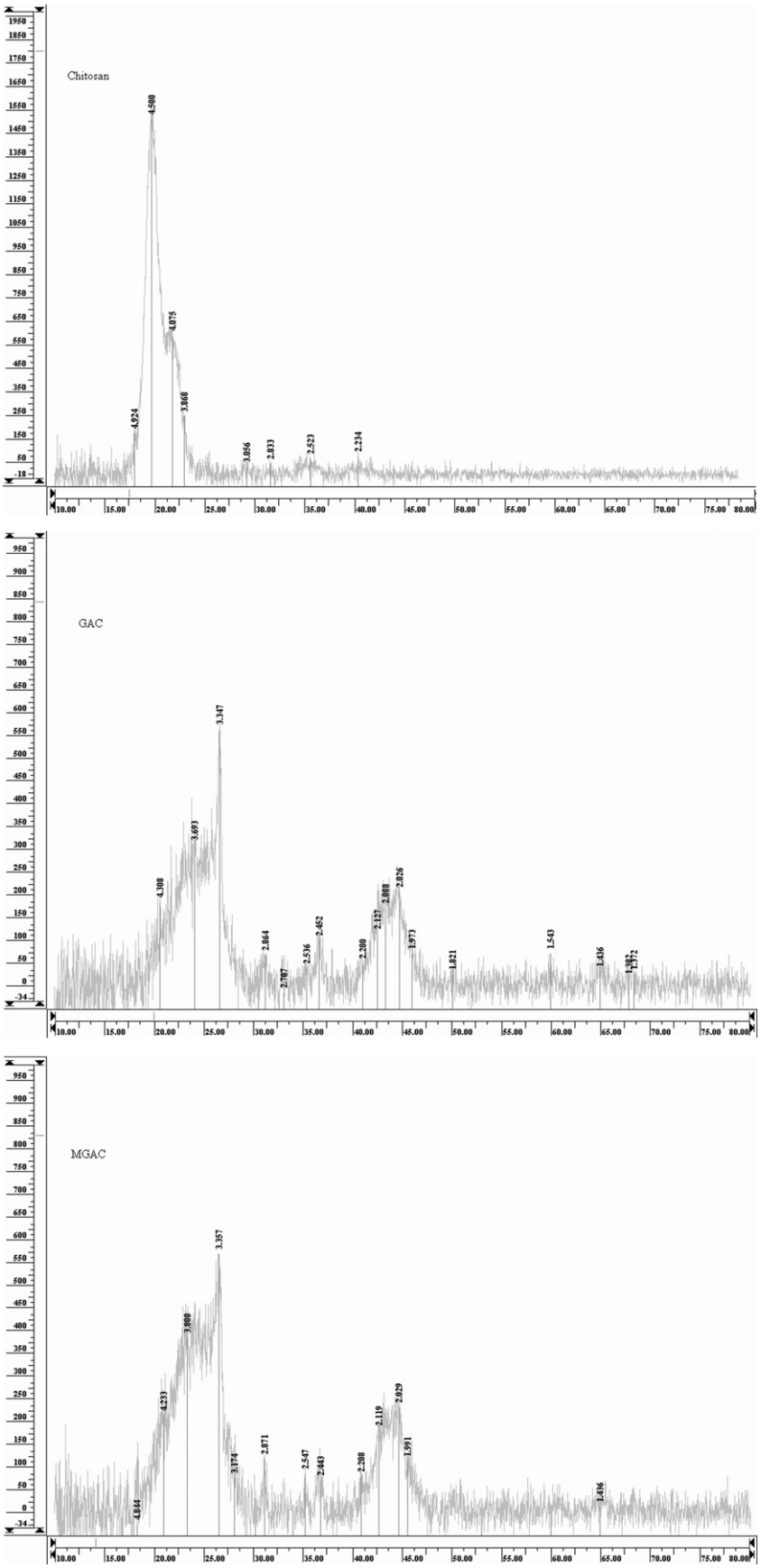

Fig. 2. X-ray spectrum for the GAC before and after treating by chitosan.

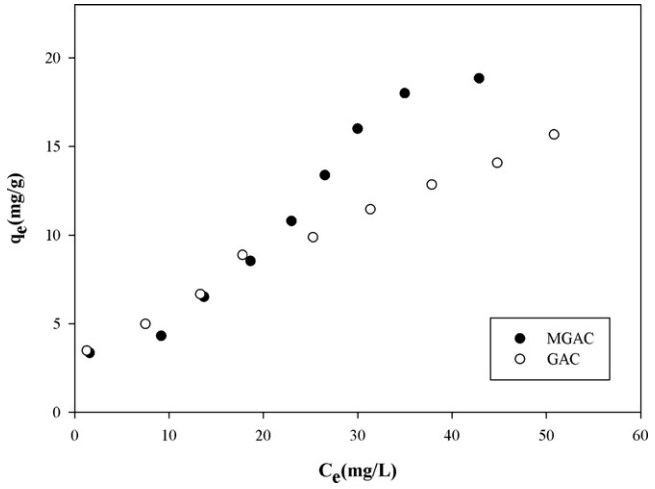

Fig. 3. Adsorption of HA onto GAC and MGAC.

at 25 °C. At pre-determined time intervals, portions of the mixture were drawn by a syringe and then centrifuged and the HA concentration was determined as described before.

3. Results and discussion

3.1. Characterization of the adsorbents by FTIR and XRD

FTIR and X-ray diffraction analysis of the adsorbents have been conducted. It is obvious from Fig. 1 that the peaks with respect to the –CH stretching, amide and amine group in chitosan have appeared at wave numbers 2925 cm^{-1}, 1650 cm^{-1} and 1590 cm^{-1} respectively. The conferred peaks can be distinguished in the spectrum of MGAC not in GAC. The X-ray diffractogram for chitosan, GAC and MGAC is shown in Fig. 2. The peak existed at $2\theta = 20^\circ$ and is a characteristic peak for chitosan. On the other hand, GAC shows its characteristic peaks at $2\theta = 26.5^\circ$ as a sharp one and at $2\theta = 24^\circ$ and 43.5° as wide peaks. By treating the GAC with chitosan, changes in X-ray diagram can be found easily in Fig. 2 where the characteristic peaks at $2\theta = 24^\circ$ is more intense. This could be proposed to the adsorbed chitosan polymers onto the GAC structure causing diffraction at $2\theta = 20^\circ$ and sheltering.

3.2. Adsorption isotherm studies

Equilibrium surface loading, q_e, was computed from the mass balance equation for each isotherm bottle using Eq. (1):

$$q_e = \frac{V(C_i - C_e)}{w} \quad (1)$$

where V is the volume of solution used in the adsorption experiment (L), C_i and C_e are the initial and equilibrium concentrations of the adsorbate (mg/L), respectively, and w is the dry weight of adsorbent (g). Fig. 3 represents the adsorption of HA on GAC and MGAC at 25 °C.

The obtained experimental equilibrium adsorption data (Fig. 3) were then compared with the adsorption isotherm models. Three models of Langmuir [35], Freundlich [36], and Tempkin [37] in their related linearized expressions have been used as Eqs. (2), (3) and (4) respectively

$$\frac{1}{q_e} = \frac{1}{K_L C_e} + \frac{a_L}{K_L} \quad (2)$$

where C_e is the concentration of adsorbate (mg/L) at equilibrium, q_e the amount of adsorbate at equilibrium (mg/g), a_L (L/mg) and K_L (L/g), are constants

$$\log q_e = \log K_f + \frac{\log C_e}{n} \quad (3)$$

where K_f ((mg/g) $(mg/L)^{-1/n}$) and n are constants incorporating all factors affecting the adsorption process such as adsorption capacity and intensity. If n is close to 1, the surface heterogeneity could be assumed to be less significant and as n approaches 10 the impact of surface heterogeneity becomes more significant [38].

$$q_e = B \ \ln A + B \ln C_e \quad (4)$$

where B and A (L/g) are the Tempkin constants and can be determined by a plot of q_e versus $\ln C_e$.

Parameters related to each isotherm were determined by using linear regression analysis and the square of the correlation coefficients (R^2) have been calculated. A list of the parameters obtained along with R^2 values is provided in Table 1 for HA adsorption onto the GAC and MGAC.

Fig. 3 revealed that the adsorption capacity of MGAC has increased for HA. It is hypothesized that after chitosan treatment, chemisorption is taking place; hence more adsorbate can bind to the adsorbent. It can be related to the amine functional group in chitosan structure where the desirable chemical binding such as electrostatic attraction can occur between HA and chitosan. This excess adsorption is obvious at higher concentration of HA where more contingency of chemical binding existed.

Comparing the calculated correlation coefficients in Table 1 showed that all investigated isotherm models are reasonable fitted to the equilibrium data for HA adsorption on MGAC and GAC. Since n values for Freundlich equation are close to 1 for both adsorbents, the surface heterogeneity could be assumed to be less significant [39]. On the other hand, Langmuir equation describes adsorption on strongly homogeneous surfaces. This is confirmed by previous description of n values in Freundlich equation. Based on this reason it can be seen from the obtained data that Langmuir equation can be fitted with a desirable $R^2 = 0.99$ with a monolayer capacity (K_L/a_L) of 55.8 mg/g and 71.4 mg/g for GAC and MGAC, respectively.

It is difficult to predict the adsorption behaviour of HA because little is known about its precise molecular structure. A study on the adsorption of HAs and other dissolved organic material has shown that not only the molecular size and chemical characteristic of macromolecules but also the pH and ionic strength of solution and the porous texture of adsorbent have an influence on the extent of their removal [40]. Amino ($-NH_2$) and hydroxyl (–OH) groups in chitosan structure provide coordination and reaction sites. Chitosan surface can be positively charged in acidic solutions. The adsorption of HA onto the MGAC may be hypothesized as consisting of two processes: (a) transport of HA from the bulk solution to the surface of the adsorbate and then (b) attachment of HA to the outside layer chitosan of the GAC and diffusing concurrently into

Table 1
Regression parameters for the different adsorption isotherm equations.

Adsorbent	Langmuir			Freundlich			Tempkin		
	R^2	K_L (L/g)	a_L (L/mg)	R^2	K_f (mg/g) $(mg/L)^{-1/n}$	n	R^2	A (L/g)	B
GAC	0.99	0.826	0.0148	0.98	1.091	1.251	0.97	0.189	9.917
MGAC	0.99	0.986	0.0138	0.99	1.259	1.222	0.96	0.255	9.831

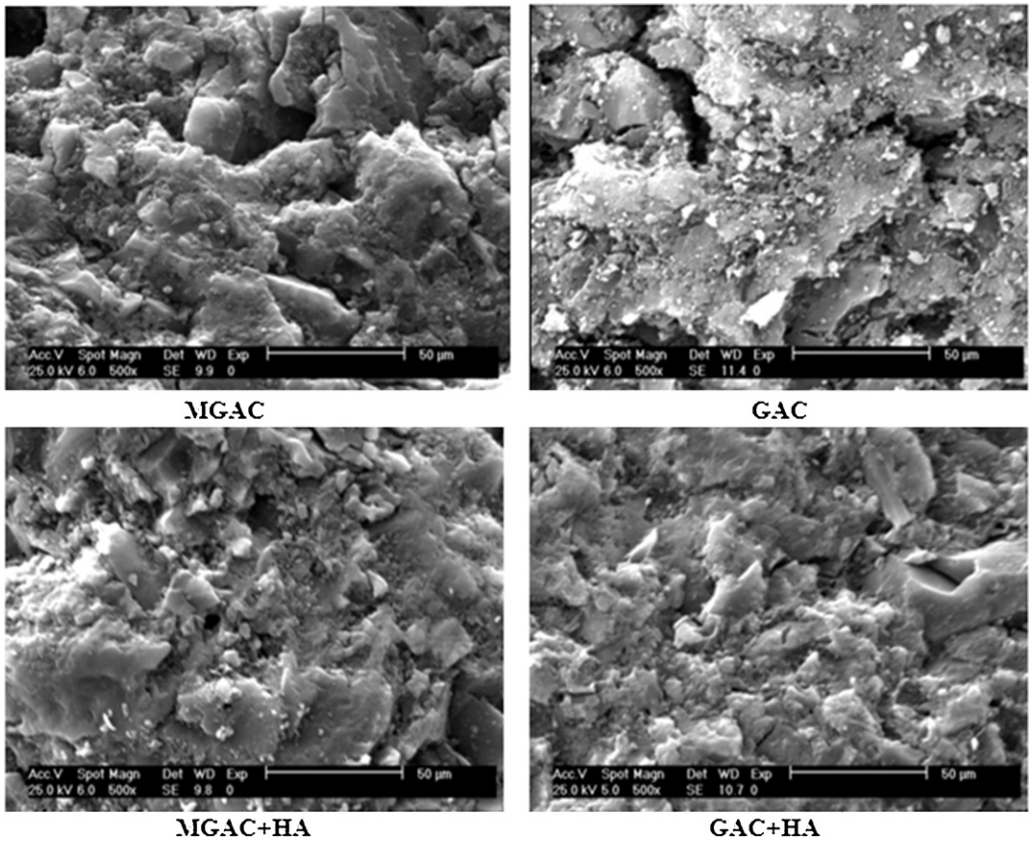

Fig. 4. SEM photograph of GAC and MGAC before and after adsorption.

the pores. In the initial stage, the surface of GAC is relatively free of humic acid and the humic acid molecules that arrive at the surfaces may attach instantly to the protonated amino groups ($-NH_3^+$) of the chitosan.

3.3. SEM studies

SEM technique was applied in order to confirm the adsorption of chitosan on GAC, the adsorption of HA on the adsorbents, and to get more information regarding to the distinction of the adsorbents surface morphology after the treatment. The images are shown in Fig. 4. It can be seen that the surface of the GAC was coarse with crispy appearance and sharp edges. It can be clearly observed that the GAC, after chitosan adsorption loses its rough structure and gain more smooth surface containing blunt edges. The photograph of the adsorbates also shows blocking of holes due to the adsorption of HA in the porous region of carbon.

3.4. Effect of pH on the adsorption

The effect of pH on the adsorption of HA onto GAC and MGAC, has been investigated.

It can be seen from Figs. 5 and 6 that the amount of adsorption increased by decreasing the pH of solution. As known, the charge

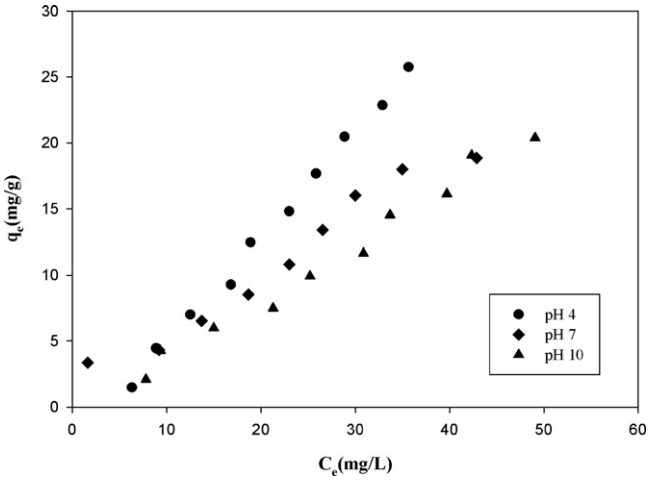

Fig. 5. Adsorption of HA onto MGAC at different pH.

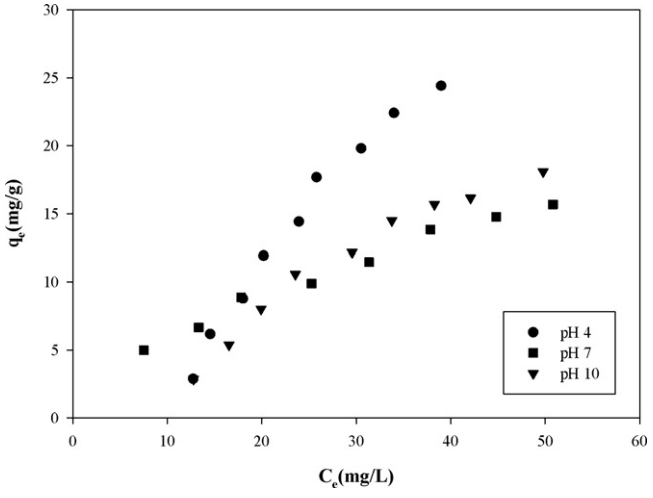

Fig. 6. Adsorption of HA onto GAC at different pH.

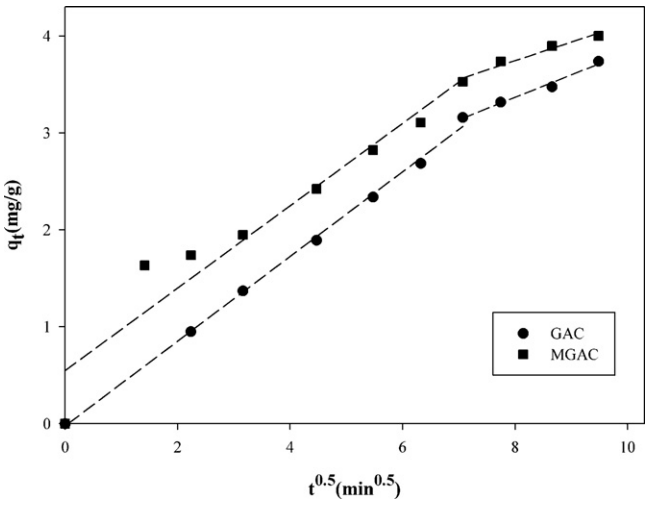

Fig. 7. Intra-particle diffusion plot for HA adsorption onto GAC and MGAC.

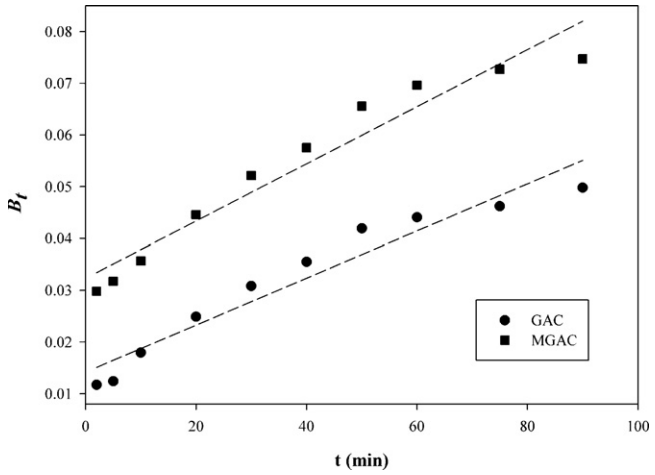

Fig. 8. Correlationship of B_t versus t for HA adsorption onto GAC and MGAC.

of HA molecules changes with pH. Carboxylic and phenolic groups have the highest contribution to the charge of HA molecules. The dissociation of carboxylic groups takes place at pH greater than 4 whereas the phenolic groups undergo dissociation at pH greater than 8. Hence, with increasing the pH of solution the negative charge of HA molecules also increase. Taking into consideration that the electrostatic forces affect the adsorption process significantly [40], an electrostatic repulsion between neighbouring negatively charged sites cause stretching out of the HA molecules which is decreased with decreasing pH and as a result, HA molecules may become smaller in size due to the tendency to coil. Therefore, it has been suggested that humic acid may exist in a spherical structure at lower pH but can exist in a rather linear or stretched structure at higher pH. Hence, an increase in the sizes of humic acid macromolecules with increasing the solution pH values can be another factor contributing to the lower adsorption capacity at higher pH. However, the hydrogen bonds can be formed between the coiled molecules which leads to the formation of aggregates of a larger size compared to that of single HA molecule [32,40]. On the other hand, some of physico-chemical properties of chitosan which determine its potential as biosorbent are depend on the chain length, charge density and distribution regarding its cationic nature coming from degree of deacetylation. At neutral pH, about 50% of total amine groups remain protonated and theoretically available for the adsorption. As the pH decreases, the protonation of amine groups increases leading to more adsorption efficiency [29]. It is clear that adsorption of HA on the MGAC also involves the protonation of the amino groups in chitosan following to form complexes with HA negative moieties. The adsorption capacity can, therefore, be expected to increase if the amount of protonated amino groups increases [32]. It can be expected that the adsorption of HA onto GAC and MGAC decreases by raising the pH. Fig. 5 reveals the consistency between the theories and experimental. On the other hand the GAC which has pH_{PZC} 9.8, it, therefore has an appropriate tendency for the adsorption of HA below this pH (Fig. 6). As a result it is obvious from Figs. 5 and 6 that the maximum adsorption has been occurred at pH 4 for the adsorbents.

3.5. Kinetic studies

The kinetic adsorption data were evaluated to understand the dynamics of the adsorption reaction in terms of the order of the rate constant. Batch experiments were conducted to explore the rate of HA adsorption by GAC and MGAC as described in Section 2.3 at pH 7. Three kinetic models were applied to the adsorption kinetic data in order to investigate the behaviour of adsorption process of HA onto the absorbents. These models include the pseudo-first-order kinetics (reversible or irreversible) [41], the pseudo-second-order [42] and the intraparticle diffusion models [38]. The linear form of reversible pseudo-first-order model can be formulated as:

$$\ln(q_e - q_t) = \ln\ q_e - K_1 \times t \tag{5}$$

where q_e (mol/g) and q_t (mol/g) are the amount of HA adsorbed at equilibrium and at time t, respectively, and K_1 (min^{-1}) is the rate constant. K_1 values were evaluated from the linear regression of $\ln(q_e - q_t)$ versus t data.

Linear form of irreversible pseudo-first-order model can be formulated as:

$$\ln\left(\frac{C_0}{C_t}\right) = K \times t \tag{6}$$

where C_0 (mg/L) is the initial concentration of HA and C_t (mg/L) is equilibrium concentration of HA at time t respectively, and K (min^{-1}) is the rate constant. Evaluation of data has been done using linear plot of $\ln(C_0/C_t)$ versus time.

The linear form of pseudo-second-order equation can be formulated as:

$$\frac{t}{q_t} = \frac{1}{K_2 q_e^2} + \frac{t}{q_e} \tag{7}$$

where q_e and q_t are surface loading of HA at equilibrium and time t respectively, and K_2 (g/mg min) is the second-order rate constant.

Table 2
Calculated parameters for the studied adsorption kinetics at 25 °C.

Adsorbent	Pseudo first order				Pseudo second order		
	Irreversible		Reversible		$K_2 q_e^2$ (mg/ g min)	K_2 (g/min mg)	R^2
	K (min^{-1})	R^2	K_1 (min^{-1})	R^2			
GAC	0.002	0.95	0.00045	0.94	0.282	0.017	0.95
MGAC	0.002	0.95	0.00055	0.94	0.501	0.028	0.98

The linear plot of t/q_t as a function of t provided not only the rate constant K_2, but also an independent evaluation of q_e.

The fitting of experimental data to the pseudo-first-order and the pseudo-second-order equations seemed to be quite good for GAC where the calculated correlation coefficients (R^2) showed almost the same values (Table 2).

For adsorption of HA onto MGAC, the obtained results represent more conformity to pseudo-second-order model ($R^2 = 0.98$). The initial adsorption rate, $K_2 q_e^2$, for MGAC (0.028 mg/min g) is greater than for GAC (0.017 mg/min g). This can be explained by chitosan potential to adsorb HA molecules excess to GAC through electrostatic attraction between amine group and negative functional groups in HA structure.

Kinetic data for the adsorption of HA were also analyzed according to intraparticle diffusion model which can be formulated as:

$$q_t = k_p t^{0.5} \tag{8}$$

where q_t is the amount of HA adsorbed (mg/g) at time t, and k_p (mg/g min$^{0.5}$) is the rate constant for intra-particle diffusion. Results are shown in Fig. 7. Usually the plot of q_t versus $t^{0.5}$ may be distinguished in two or more steps taking place during adsorption process including instantaneous adsorption stage by external mass transfer (first sharper portion), intra-particle diffusion which is the rate controlling stage (second portion as the gradual adsorption stage) and the final equilibrium stage where the intra-particle diffusion starts to slow down due to the extremely low solute concentration in solution (the third portion) [43].

From Fig. 7, two straight lines can be diagnosed for both adsorption systems. The first line with steeper slope corresponds to film and pore diffusion taking place simultaneously in the adsorption systems. The slope of this linear portion, k_p (0.2321 mg/g min$^{0.5}$ for GAC and 0.1916 mg/g min$^{0.5}$ for MGAC) can be defined as a rate parameter and characteristic of the rate of adsorption in the region where intra-particle diffusion is occurring. Declining of the second linear portion is dealing with the diminishing of intra-particle diffusion and reaching equilibrium.

Since the intercept of the plot of q_t versus $t^{0.5}$ for MGAC is not equal to zero, the actual rate-controlling step involved in the HA adsorption process, has been further analyzed using Eqs. (9)–(11) [44]

$$F = 1 - \frac{6}{\pi^2} \exp(-B_t) \tag{9}$$

where F is the fraction of adsorbate adsorbed at different times t and B_t is a mathematical function of F and F can be expressed as

$$F = \frac{q_t}{q_e} \tag{10}$$

where q_t and q_e represent the amount adsorbed (mg/g) at any time t and at infinite time. Substituting Eq. (9) into Eq. (10), the kinetic expression becomes

$$B_t = -0.4977 - \ln\left(1 - \frac{q_t}{q_e}\right) \tag{11}$$

where q_t and q_e represent the amount adsorbed (mg/g) at any time t and at infinite time. B_t is a mathematical function of q_t/q_e.

The calculated B_t values were plotted against time as shown in Fig. 8. The linearity of this plot will provide useful information for distinguishing between film diffusion and intra-particle diffusion rates of adsorption. If a plot of B_t versus t is a straight line passing through the origin, then adsorption will be governed by a particle-diffusion mechanism, otherwise governed by film diffusion [45]. It can be seen from Fig. 8 that film diffusion may govern the rate-limiting process for MGAC. It is postulated that the HA was transported onto the external surface of the adsorbent through film diffusion with the fastest rate. After saturation of the surface, the HA molecule penetrate into the GAC and MGAC by intra-particle diffusion through pore and interior surface diffusion until equilibrium is attained. As a consequence the adsorption data indicate that the removal of HA from aqueous solution using MGAC is rather a complex process, involving both boundary layer and intra-particle diffusion.

4. Conclusion

Equilibrium adsorption of HA on GAC before and after treating by chitosan has been investigated. The equilibrium data have been explored by Freundlich, Langmuir and Tempkin adsorption models. The parameters of each isotherm have been determined. The results showed that the experimental data could be correlated by Langmuir adsorption isotherm where monolayer surface loading was calculated to be 71.4 mg/g, for MGAC. The most adsorption capacity was found to occur at pH 4 where the probability of electrostatic bond formation between chitosan and HA molecules is increased. Kinetic studies showed that the initial rate of adsorption is increased by chitosan treatment of GAC and pseudo second order model could be correlated to the obtained data. Results revealed that MGAC has significantly removed HA from aqueous solutions. In MGAC, chitosan provides chemical binding whereby the adsorption will not follow predominantly by physical adsorption mechanism.

References

[1] M. Salman, B. El-Eswed, F. Khalili, Adsorption of humic acid on bentonite, Appl. Clay Sci. 38 (2007) 51–56.
[2] A.I. Zouboulis, W. Jun, I.A. Katsoyiannis, Removal of humic acids by flotation, Colloids Surf. A 231 (2003) 181–193.
[3] S. Wang, Z.H. Zhu, Humic acid adsorption on fly ash and its derived unburned carbon, J. Colloid Interf. Sci. 315 (2007) 41–46.
[4] A.S. Koparal, Y.S. Yildiz, B. Keskinler, N. Demircioglu, Effect of initial pH on the removal of humic substances from wastewater by electrocoagulation, Sep. Purif. Technol. 59 (2008) 175–182.
[5] S. Wang, T. Terdkiatburana, M.O. Tadé, Single and co-adsorption of heavy metals and humic acid on fly ash, Sep. Purif. Technol. 58 (2008) 353–358.
[6] W.J. Hung, H.H. Yeh, Reaction of chlorine with NOM adsorbed on powdered activated carbon, Water Res. 33 (1) (1999) 65–72.
[7] A. Alpatova, S. Verbych, M. Bryk, R. Nigmatullin, N. Hilal, Ultrafiltration of water containing natural organic matter: heavy metal removing in the hybrid complexation–ultrafiltration process, Sep. Purif. Technol. 40 (2004) 155–162.
[8] R. Gong, M. Li, C. Yang, Y. Suna, J. Chenb, Removal of cationic dyes from aqueous solution by adsorption on peanut hull, J. Hazard. Mater. B121 (2005) 247–250.
[9] J. Wiszniowski, D. Robert, J. Surmacz-Gorska, K. Miksch, S. Malato, J.V. Weber, Solar photocatalytic degradation of humic acids as a model of organic compounds of landfill leachate in pilot-plant experiments: influence of inorganic salts, Appl. Catal. B: Environ. 53 (2004) 127–137.
[10] H.J. Kim, K. Baek, B.K. Kim, J.W. Yang, Humic substance-enhanced ultrafiltration for removal of cobalt, J. Hazard. Mater. A 122 (2005) 31–36.
[11] B. Seredyńska-Sobecka, M. Tomaszewska, A.W. Morawski, Removal of humic acids by the ozonation–biofiltration process, Desalination 198 (2006) 265–273.
[12] C.Y. Tang, Y.N. Kwon, J.O. Leckie, Fouling of reverse osmosis and nanofiltration membranes by humic acid—Effects of solution composition and hydrodynamic conditions, J. Membr. Sci. 290 (2007) 86–94.
[13] Q. Ji, H. Liu, C. Hu, J. Qu, D. Wang, J. Li, Removal of disinfection by-products precursors by polyaluminum chloride coagulation coupled with chlorination, Sep. Purif. Technol. 62 (2008) 464–469.
[14] H. Baker, F. Khalili, Comparative study of binding strengths and thermodynamic aspects of Cu(II) and Ni(II) with humic acid by Schubert's ion-exchange method, Anal. Chim. Acta 497 (2003) 235–248.
[15] H. Baker, F. Khalili, A study of complexation thermodynamic of humic acid with cadmium (II) and zinc (II) by Schubert's ion-exchange method, Anal. Chim. Acta 542 (2005) 240–248.
[16] C. Senem Uygunera, S. Altan Suphandaga, A. Kercb, M. Bekboleta, Evaluation of adsorption and coagulation characteristics of humic acids preceded by alternative advanced oxidation techniques, Desalination 210 (2007) 183–193.
[17] P.K. Malik, Use of activated carbons prepared from sawdust and rice-husk for adsorption of acid dyes: a case study of Acid Yellow 36, Dyes Pigm. 56 (2003) 239–249.
[18] J. Duan, F. Wilson, N. Graham, J. Hwa Tay, Adsorption of humic acid by powdered activated carbon in saline water conditions, Desalination 151 (2002) 53–66.
[19] T. Terdkiatburana, S. Wang, M.O. Tade, Competition and complexation of heavy metal ions and humic acid on zeolitic MCM-22 and activated carbon, Chem. Eng. J. 139 (2008) 437–444.

[20] T.S. Anirudhan, M. Ramachandran, Surfactant-modified bentonite as adsorbent for the removal of humic acid from wastewaters, Appl. Clay Sci. 35 (2007) 276–281.
[21] S. Vreysen, A. Maes, Adsorption mechanism of humic and fulvic acid onto Mg/A layered double hydroxides, Appl. Clay Sci. 38 (2008) 237–249.
[22] L. Zhao, F. Luo, J.M. Wasikiewicz, H. Mitomo, N. Nagasawa, Y. Toshiaki, M. Tamada, F. Yoshii, Adsorption of humic acid from aqueous solution onto irradiation-crosslinked carboxymethyl chitosan, Bioresour. Technol. 99 (2008) 1911–1917.
[23] N. Koryabkina, J.A. Bergendahl, R.W. Thompson, A. Giaya, Adsorption of disinfection byproducts on hydrophobic zeolites with regeneration by advanced oxidation, Micropor. Mesopor. Mater. 104 (2007) 77–82.
[24] T. Moriguchi, K. Yano, M. Tahara, K. Yaguchi, Metal-modified silica adsorbents for removal of humic substances in water, J. Colloid Interf. Sci. 283 (2005) 300–310.
[25] F. Hua-Jun, H. Li-Fang, M. Qaisar, L. Yan, S. Dong-Sheng, Study on biosorption of humic acid by activated sludge, Biochem. Eng. J. 39 (2008) 478–485.
[26] A.F.Y. Adou, V.S. Muhandiki, Y. Shimizu, S. Matsui, A new economical method to remove humic substances in water: adsorption onto a recycled polymeric material with surfactant addition, Water Sci. Technol. 43 (2001) 1–7.
[27] M.N.V. Ravi Kumar, A review of chitin and chitosan applications, React. Funct. Polym. 46 (2000) 1–27.
[28] M. Rinaudo, Chitin and chitosan: properties and applications, Prog. Polym. Sci. 31 (2006) 603–632.
[29] G. Crini, P.M. Badot, Application of chitosan, a natural aminopolysaccharide, for dye removal from aqueous solutions by adsorption processes using batch studies: a review of recent literature, Prog. Polym. Sci. 33 (2008) 399–447.
[30] S. Chatterjee, S. Chatterjee, B.P. Chatterjee, A.K. Guha, Adsorptive removal of congo red, a carcinogenic textile dye by chitosan hydrobeads: binding mechanism, equilibrium and kinetics, Colloids Surf. A 299 (2007) 146–152.
[31] W. Po Cheng, F. Hwa Chi, A study of coagulation mechanisms of polyferric sulfate reacting with humic acid using a fluorescence-quenching method, Water Res. 36 (2002) 4583–4591.
[32] X. Zhang, R. Bai, Mechanisms and kinetics of humic acid adsorption onto chitosan-coated granules, J. Colloid Interf. Sci. 264 (2003) 30–38.
[33] B. Noroozi, G.A. Sorial, H. Bahrami, M. Arami, Adsorption of binary mixtures of cationic dyes, Dyes Pigm. 76 (2008) 784–791.
[34] M.V. Lopez-Ramon, F. Stoeckli, C. Moreno-Castilla, F. Carrasco-Marin, On the characterization of acidic and basic surface sites on carbons by various techniques, Carbon 37 (1999) 1215–1221.
[35] I. Langmuir, The constitution and fundamental properties of solids and liquids, J. Am. Chem. Soc. 38 (1916) 2221–2295.
[36] H.M.F. Freundlich, Uber die adsorption in losungen, Z. Phys. Chem. 57 (1906) 385–471.
[37] M.J. Tempkin, V. Pyzhev, Acta Physiol. Chem. USSR 12 (1940) 217–222.
[38] B. Noroozi, G. Sorial, A.H. Bahrami, M. Arami, Equilibrium and kinetic adsorption study of a cationic dye by a natural adsorbent-silkworm pupa, J. Hazard. Mater. B139 (2007) 167–174.
[39] M.M. Dávila-Jiménez, M.P. Elizalde-González, A.A. Peláez-Cid, Adsorption interaction between natural adsorbents and textile dyes in aqueous solution, Colloids Surf. A 254 (2005) 107–114.
[40] E. Lorenc-Grabowska, G. Gryglewicz, Adsorption of lignite-derived humic acids on coal-based mesoporous activated carbons, J. Colloid Interf. Sci. 284 (2005) 416–423.
[41] M.Y. Chang, R.S. Juang, Equilibrium and kinetic studies on the adsorption of surfactant, organic acids and dyes from water onto natural biopolymers, Colloids Surf. A. 269 (2005) 35–46.
[42] F.C. Wu, R.L. Tseng, S.C. Huang, R.S. Juang, Characteristics of pseudo-second-order kinetic model for liquid-phase adsorption: a mini-review, Chem. Eng. J. 151 (2009) 1–9.
[43] Q. Sun, L. Yang, The adsorption of basic dyes from aqueous solution on modified peat-resin particle, Water Res. 37 (2003) 1535–1544.
[44] G.E. Boyd, A.W. Adamson, L.S. Meyers, The exchange adsorption of ions from aqueous solution by organic zeolites. II. Kinetics, J. Am. Chem. Soc. 69 (1947) 2836–2848.
[45] S. Wang, H. Li, L. Xu, Application of zeolite MCM-22 for basic dye removal from wastewater, J. Colloid Interf. Sci. 295 (2006) 71–78.